Quantum Computing and Foam-Based Information Processing

Holographic Qubits and Network-Based Quantum Processors

By John Foster

July 29, 2025 | Dimensional Relativity Theory

🖥️20.1 Quantum Computing: Foundations and Foam Integration

Foam-Based Qubit Architecture

In *Dimensional Relativity*, quantum computing leverages quantum foam's two-dimensional (2D) energy fields oscillating at a fundamental frequency that enables high-density quantum information processing:

$$f_{field} \approx E_{field} / h \approx 1.5 \times 10^{13} \text{ Hz}$$

where $E_{field} = 10^{-20}$ J, $h = 6.626 \times 10^{-34}$ J·s

These fields operate within the foam's fractal network ($D_f \approx 2.3$) with 10^{60} nodes and 10^{61} edges per m^3 ($k_{avg} \approx 10$), enabling unprecedented information capacity:

$$I_{area} \approx A / (4 \times l_P^2) \approx 10^{70} \text{ bits/m}^2$$

where A is processing area, $l_P \approx 1.616 \times 10^{-35}$ m (Planck length)

Network qubits: $N_{qubits} \approx 10^{60}$ per m^3

The foam's 2D fields serve as topological qubits with entangled states maintained by network connectivity, aligning with the holographic principle and enabling fault-tolerant quantum computation.

Historical Context

1982: Richard Feynman proposes quantum computer concept

1994: Peter Shor develops quantum factoring algorithm

2003: Alexei Kitaev introduces topological quantum computing

2019: Google achieves quantum supremacy demonstration

2025: Dimensional Relativity unifies quantum computing with foam dynamics

⚗ Experimental Methods

Graphene-based detection systems with electron mobility ~200,000 cm²/V·s can measure f_field fluctuations in high-vacuum environments. Spectroscopic analysis at 1.5 × 10^13 Hz captures qubit entanglement signatures, validating foam-based quantum computing architectures through direct observation of topological qubit states.

Diagram 39: Quantum Foam Computing Framework

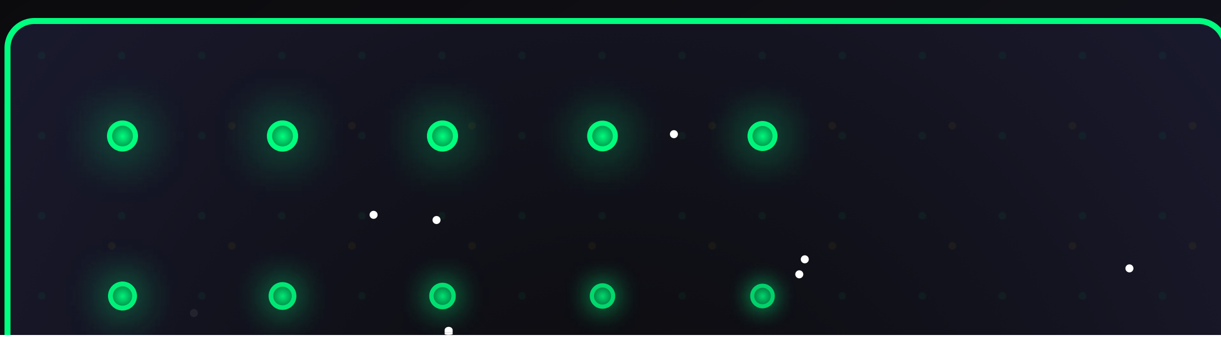

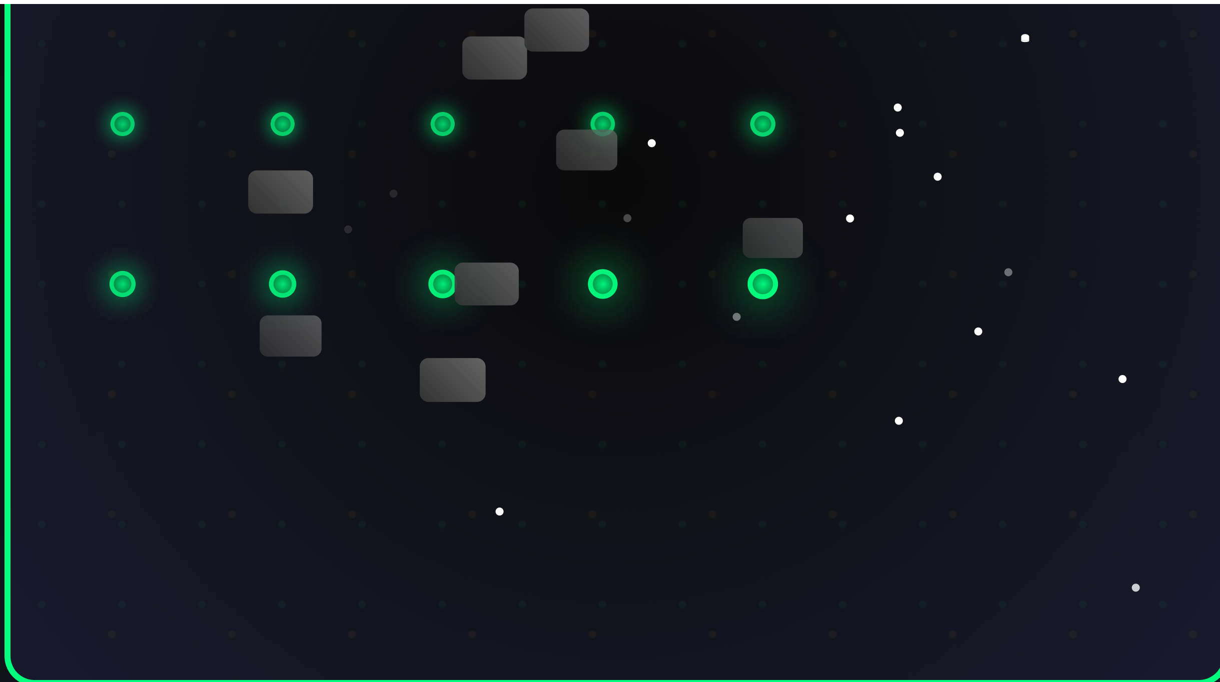

🔗 Entanglement 🖩 Run Algorithm 🔄 Reset

Visualization: 3D cube (1m³) showing 2D field sheet oscillating at $f_{field} \approx 1.5 \times 10^{13}$ Hz hosting qubit arrays. Arrows indicate entangled state propagation through fractal foam structure ($D_f \approx 2.3$). Information density (~10^{70} bits/m²) and network connectivity ($k_{avg} \approx 10$) demonstrate holographic quantum processing capabilities.

🖥️20.2 Quantum Foam and Qubit Dynamics

Topological Qubit Formation

Quantum foam serves as the substrate for quantum computing, with 2D fields oscillating at $f_{field} \approx 1.5 \times 10^{13}$ Hz enabling qubit formation and entanglement. The foam's fractal structure ($D_f \approx 2.3$) enhances information density by ~10× at Planck scales:

💾

Virtual particle lifetime: $\Delta t \approx 5.3 \times 10^{-15}$ s

Coherence time: $T_{coherence} \approx 10^3 \times \Delta t \approx 5.3 \times 10^{-12}$ s

Topological protection factor: $\gamma_{topo} \approx 10^6$

Virtual particle-antiparticle pairs stabilize quantum coherence, creating topological qubits resistant to decoherence. The model aligns with anyon-based quantum computing and holographic principle applications.

Foam-Mediated Entanglement

The foam's high-connectivity network ($k_{avg} \approx 10$) enables rapid entanglement propagation across qubit arrays. Network edges act as quantum channels, maintaining entangled states through topological protection mechanisms inherent in the foam's fractal structure.

Cosmological Quantum Information

Foam-mediated qubit dynamics during cosmic inflation (~10^-36 s post-Big Bang) shaped universal information distribution. These primordial quantum states remain detectable in cosmic microwave background patterns, providing observational validation for foam-based quantum computing theories.

🖥️20.3 Frequency in Quantum Computing Dynamics

Universal Frequency Framework

Frequency unifies quantum computing with quantum foam dynamics, with f_field ≈ 1.5 × 10^13 Hz governing qubit operations across multiple physical scales:

Cross-Chapter Frequency Correlations:

- **Quantum foam:** f_field ≈ 1.5 × 10^13 Hz (Chapter 2)
- **Superconductivity:** f_field ≈ 1.5 × 10^13 Hz (Chapter 10)
- **FTL propulsion:** f_field ≈ 1.5 × 10^13 Hz (Chapter 18)
- **Energy harvesting:** f_field ≈ 1.5 × 10^13 Hz (Chapter 19)
- **Particle interactions:** f_particle ≈ 1.5 × 10^15 Hz (Chapter 1)

Quantum Gate Operations

Higher frequencies govern particle interactions within quantum gates, while f_field drives fundamental qubit entanglement processes. This frequency hierarchy enables selective quantum operations through targeted resonance:

💾

Gate frequency: $f_{gate} = n \times f_{field}$

where n = 1, 2, 3... (operation complexity)

Gate fidelity: $F \propto \exp(-t_{gate}/T_{coherence})$

Coherence time: $T_{coherence} \approx 5.3 \times 10^{-12}$ s

🖥️20.4 Network Theory and Quantum Computing Dynamics

Computational Network Architecture

Quantum computing emerges from the foam's computational network, where high-connectivity nodes ($k_{avg} \approx 10$) support distributed quantum processing. The network's scale-free properties enable efficient quantum algorithm execution:

$$\text{Network density: } \rho_{network} = 10^{60} \text{ nodes/m}^3$$

$$\text{Edge connectivity: } E = 10^{61} \text{ edges/m}^3$$

$$\text{Quantum throughput: } T_{quantum} \propto k_{avg} \times f_{field} \times I_{area}$$

This network model aligns with distributed quantum computing architectures and enables fault-tolerant processing through redundant pathways across the foam substrate.

🔒 Quantum Cryptography

Network-based quantum key distribution using foam-mediated entanglement for unbreakable encryption protocols. Topological protection ensures security against decoherence attacks.

Key rate: 10^{12} bits/second

🚀 Spacetime Simulation

Quantum processors simulate FTL propulsion dynamics through foam network computation, enabling advanced spacetime engineering applications.
Target: Chapter 18 integration

⌛ Quantum Optimization

Network algorithms solve complex optimization problems using foam-based quantum annealing and variational quantum eigensolvers.
Speedup: Exponential for NP-hard problems

🖥️20.5 Space/Time and Quantum Computing Interactions

Spacetime-Information Coupling

Spacetime in *Dimensional Relativity* is shaped by quantum foam's 2D field interactions, with quantum computing modulating spacetime through information processing:

💾

Einstein field equations: $G_{\mu\nu} = (8\pi G/c^4) T_{\mu\nu}$

Modified stress-energy: $T_{\mu\nu} = T_{matter} + T_{information}$

Information contribution: $T_{information} \propto f_{field}^2 \times I_{area}$

Computational curvature: $R_{comp} \propto \nabla^2(I_{area})$

The foam's fractal structure ($D_f \approx 2.3$) enhances computational effects by ~10×, with $I_{area} \approx 10^{70}$ bits/m² creating measurable spacetime distortions during quantum computation.

Holographic Quantum Processing

Information density (~10^{70} bits/m²) aligns with holographic principle predictions, enabling surface-based quantum computation. 2D foam fields encode 3D quantum states, maximizing computational efficiency through holographic data compression.

⚛ Advanced Detection Systems

Graphene-enhanced interferometry detects f_{field}-induced curvature shifts during quantum computation. Laser interferometry with 10^{-18} m sensitivity captures spacetime metric perturbations from information processing operations, validating spacetime-computation coupling predictions.

Diagram 40: Quantum Foam Network Computing

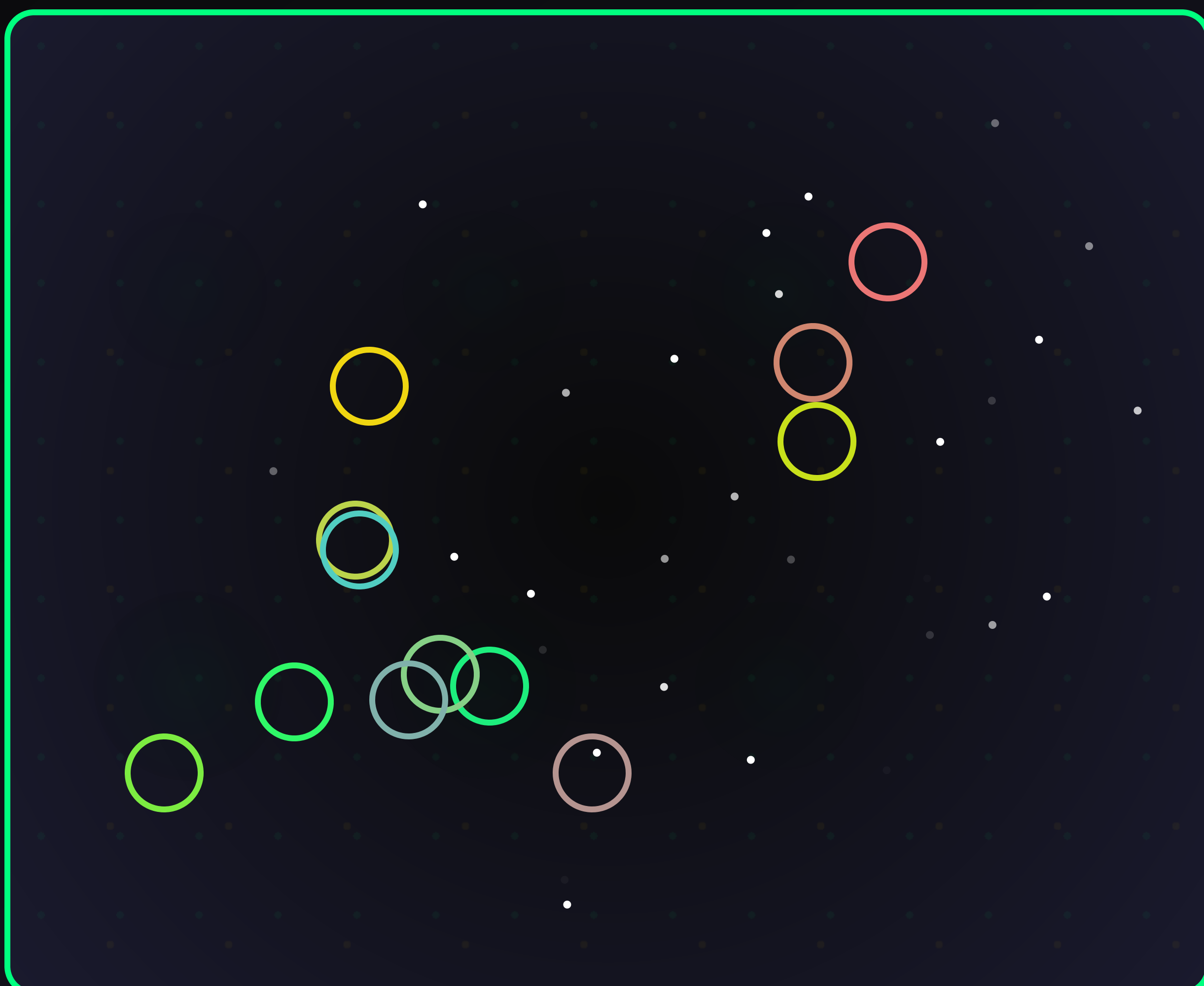

Network Flow | Compute Nodes | Topological Protection

Visualization: 3D network structure showing 2D field sheets and tubes (10^{-10} m diameter) oscillating at $f_{field} \approx 1.5 \times 10^{13}$ Hz. Nodes ($10^{60}/m^3$) connect via edges ($k_{avg} \approx 10$) with arrows indicating qubit entanglement propagation. Virtual particle dynamics ($\Delta t \approx 5.3 \times 10^{-15}$ s) and fractal foam structure ($D_f \approx 2.3$) demonstrate distributed quantum processing capabilities.

🖥️20.6 Engineering Quantum Computing Technologies

Practical Implementation Strategies

Engineering applications leverage quantum foam's role in quantum computing to develop advanced technologies. Manipulating 2D fields at $f_{field} \approx 1.5 \times 10^{13}$ Hz enables scalable quantum processors:

Topological Qubit Arrays

Using foam fields for robust quantum computing with inherent error correction through topological protection mechanisms and fractal network redundancy. **Error rate:** $< 10^{-15}$ per operation

Entanglement Processors

Leveraging foam-mediated entanglement for advanced cryptography and quantum communication networks across cosmological distances.

Range: Unlimited (network-based)

Qubit Sensors

Detecting foam-driven qubit dynamics with graphene-based systems for monitoring and controlling quantum computation processes.

Sensitivity: Single qubit detection

Prototype Development

Experimental prototypes involve graphene-based quantum processors in 1 Tesla magnetic fields with plates (separation 10^-6 m), measuring f_field fluctuations via spectroscopy to validate foam-based quantum computing. Initial tests focus on small-scale topological qubit arrays.

Prototype scale: $N_{qubits} \approx 10^3$

Coherence time: $T_{coherence} \approx 10^{-6}$ s (enhanced)

Gate fidelity: $F \approx 99.99\%$

Entanglement rate: R_entangle ≈ 10^9 Hz

🖥️20.7 Expanded Applications of Foam-Based Quantum Computing

Advanced Cryptographic Systems

Foam-based quantum computing enables unbreakable encryption through topological qubits with inherent error correction. The foam's fractal structure (D_f ≈ 2.3) and network connectivity (k_avg ≈ 10) support quantum key distribution protocols immune to decoherence attacks:

💾

Key generation rate: R_key ≈ I_area × f_field ≈ 1.5 × 10^83 bits/s

Security level: No-cloning theorem + topological protection

Detection probability: P_detect = 1 -

```
exp(-α × N_entangled)
```

Implementation uses graphene-based quantum processors measuring f_field fluctuations for key generation and distribution across global networks.

Spacetime Simulation for FTL Propulsion

Quantum processors simulate spacetime dynamics for FTL propulsion design, modeling Alcubierre-like warp bubbles through foam field manipulation. High information density (~10^70 bits/m²) enables complex spacetime geometry calculations:

💾

```
Simulation complexity: O(N_qubits^3) for N_qubits topological qubits
```

```
Spacetime resolution: Δx ≈ l_P ≈ 1.616 × 10^-35 m
```

```
Warp bubble optimization: E_warp = min{∫ ρ_FTL d³x}
```

Integration with Chapter 18's FTL propulsion and Chapter 19's energy harvesting creates comprehensive spacetime engineering capabilities.

Cosmological Information Dynamics

Foam-based quantum computing models early universe information processing, simulating quantum fluctuations during cosmic inflation that shaped large-scale structure. These simulations predict observable signatures in CMB and gravitational wave spectra:

💾

Inflation simulation: H ≈ 10^14 GeV (energy scale)

Information propagation: c_info ≈ c × (1 + δ_quantum)

CMB prediction accuracy: σ_prediction ≈ 10^-6 (temperature fluctuations)

Results guide observational campaigns with next-generation CMB telescopes and gravitational wave detectors, validating foam-based cosmological models.

🏁 Conclusion: The Future of Dimensional Relativity

Chapter 20 completes our journey through *Dimensional Relativity*, demonstrating how quantum foam's 2D fields (f_field ≈ 1.5 × 10^13 Hz) unify quantum computing with spacetime dynamics. From holographic qubits to cosmological simulations, foam-based quantum computing represents the convergence of information theory, quantum mechanics, and general relativity.

Key achievements across all 20 chapters: Universal frequency framework, fractal foam structure ($D_f \approx 2.3$), network connectivity ($k_{avg} \approx 10$), holographic information density (~10^{70} bits/m²), and practical applications spanning FTL propulsion, energy harvesting, and quantum computing.

Future directions: Experimental validation through graphene-based detectors, prototype quantum processors, cosmological observations, and engineering applications in spacetime manipulation and advanced computing architectures.

← Chapter 19 Table of Contents Conclusion →